SERIES DAMPER ACTUATOR: A NOVEL FORCE/TORQUE CONTROL ACTUATOR

CHEE-MENG CHEW

Department of Mechanical Engineering, National University of Singapore, 9 Engineering Drive 1
Singapore 117576
mpeccm@nus.edu.sg

GEOK-SOON HONG

Department of Mechanical Engineering, National University of Singapore, 9 Engineering Drive 1
Singapore 117576
mpehgs@nus.edu.sg

WEI ZHOU

Department of Mechanical Engineering, National University of Singapore, 9 Engineering Drive 1
Singapore 117576
g0202537@nus.edu.sg

A novel force/torque control actuator called Series Damper Actuator (SDA) is proposed, modeled and analyzed. Compared to conventional force/torque control schemes and Series Elastic Actuator (SEA), SDA has good output force/torque fidelity, low output impedance and large force/torque range. Furthermore, varying damping coefficient endows the SDA with more advantages and makes the system more versatile. An experimental SDA system is developed, in which a Magneto-Rheological (MR) fluid damper is employed as the series damper. The experimental results show that SDA system is an effective force/torque control actuator.

Keywords: Force/torque control actuator; MR fluid damper; Series Elastic Actuator; Impedance Control; Haptic; Actuation.

1. Introduction

Force/torque control is necessary when robots need to interact with unknown environment. This is especially true for robotics system such as assembly manipulators, legged robots, haptic devices, and so on. To implement force (from here, "force" generally means "force/torque") control, a common method is to use the strain gauge setup to obtain the force signal.[1, 2, 3] The performance of this method is poor due to its low signal-to-noise ratio. Furthermore, because of its high structural stiffness, it is not suitable to be used for biomimetic legged robots or haptic devices, which require their joints to be both compliant and precisely force controlled.

Currently, the best solution for this problem is called "Series Elastic Actuator" (SEA) [4, 5] proposed by MIT leg laboratory. The key feature of this method is the introduction of a series elastic component (SEC) between the motor and the load, which consequently increases the compliance of the actuator interface. The output force f_{load} is indirectly controlled by controlling the deformation (measured by a sensor) of the elastic component, given the elastic property. Figure 1 shows a schematic diagram of the Series Elastic Actuator.

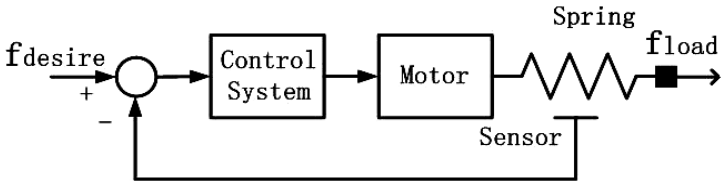

Fig. 1. Schematic diagram of Series Elastic Actuator.

The primary advantages of the SEA are good force fidelity, low output impedance, tolerance to shock loading and robust to changing loads. However, the introduction of an elastic component in the system increases the order of the system and consequently, reduces the bandwidth of the system.[6] Furthermore, the selection of the elastic property for the SEC is mainly governed by the trade-offs among the force bandwidth, force range and impact tolerance. Due to the fact that the elastic property is usually a constant (since it is difficult to achieve variable elastic property design), it is very hard to achieve good force fidelity at both low and high end range.

To overcome some of the shortcomings in the SEA, Zinn[7] proposed a force control actuation approach called Distributed Macro-Mini Actuation. The approach employs a pair of actuators which are connected in parallel. One of which is used to realize the low-frequency torque generation. The other one is for the high frequency. The resulting system can increase the force bandwidth, and yet still be able to reduce impact loads. However, the system is more complex and costlier due to the requirement of additional actuators.

In this paper, we propose a novel force control actuator system called "Series Damper Actuator" (SDA)[a].[8, 9] It has several advantages compared with the SEA system. In the following sections, the SDA system and their properties are described. The SDA system is modeled and analyzed in Section 3. Then, the control scheme of SDA is investigated in Section 4. Finally, an experiment setup is described and the experiment results and conclusion are presented.

2. Properties of Series Damper Actuator

The proposed SDA system incorporates a series damper instead of a series elastic component between the actuator and the load. A schematic diagram of the Series Damper Actuator with a feedback loop is shown in Figure 2.

[a] Patent pending.

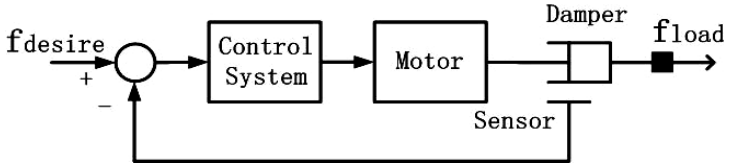

Fig.2. Schematic diagram of Series Damper Actuator.

A typical SDA system consists of a control module and two hardware modules – a motor (with or without gear transmission) and a viscous damper. The system is designed to effectively control the relative velocity in the damper to achieve the desired force given the damping coefficient. The controlled output force can be known from the following constitutive equation (for linear viscous damper):

$$F = bv \tag{1}$$

where b is the damping coefficient and v is the relative velocity in the damper.

Compared with the SEA system, the SDA uses a series damping component instead of an elastic component and, consequently, reduces the system order by one. Hence, in physical implementation, the SDA may have a larger bandwidth than the SEA system. Another advantage of the SDA system is that the damping coefficient of the damper can easily be made variable by adopting an appropriate damper design. This allows the damping coefficient to be adjusted according the environment conditions. For example, at high force and low force ranges, the damping coefficient can be increased and decreased, respectively, to allow an appropriate relative velocity in the damper. This endows the system with higher force fidelity at both high and low force ranges. Furthermore, the SDA has inherent impact absorption property due to the energy dissipation property of the series damper. This characteristic is very important for walking robots, haptic devices or robot manipulators to protect themselves from damage when they are subjected to external impact.

The main disadvantage of using damper also comes from its energy dissipation property. Such a property limits the efficiency of the SDA system.[9] In comparison, the SEA can be theoretically more efficient[4,5] due to the presence of the energy conserving elastic component. However, it is currently unclear how energy can be conserved using the elastic component when the SEA is applied to say a robotic systems like legged robots.

3. Modeling and Analysis of Series Damper Actuator

In this section, a brief investigation on the force-control properties of the Series Damper Actuator (SDA), viz. the bandwidth (fixed end) and the output impedance, is carried out. In the SDA model, we assume the damping coefficient of the series damper is constant.

3.1. *Model*

This subsection provides the model for the SDA system. The model and frequency domain block diagram for the SDA plant is shown as in Fig. 3(a) and (b), respectively. To understand the force-control properties of the SDA system, we investigate the SDA plant with a unity feedback and assume that a proportional control law is used for the feedback controller, as shown in Fig. 3(c). The adoption of such a simple control law is to enable the properties of this force-control actuator system to be clearly illustrated.

From the model, we can obtain the closed loop transfer function of the SDA system as follows:

$$F_L(s) = \frac{K_p K_b F_d(s) - K_b(J_m s + B_m)V_L(s)}{J_m s + B_m + K_b(K_p + 1)} \tag{2}$$

where K_b is the damping coefficient of the series damper; B_m is the damping coefficient experienced by the motor rotor shaft (assume viscous); V_m(s) is the motor output velocity; V_L(s) is the load velocity; K_p is the proportional gain; F_L(s) is the load force; F_d(s) is the desired output force; F_m(s) is the force applied on the motor rotor.

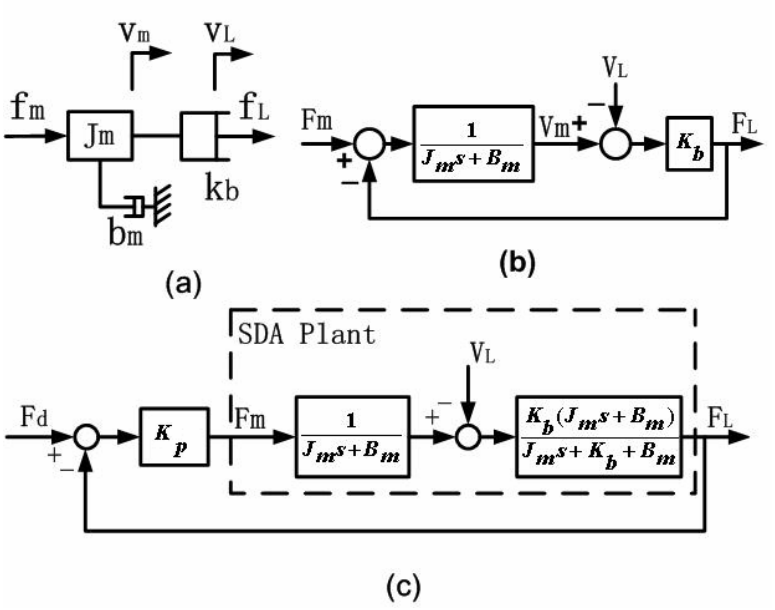

Fig. 3. (a) The SDA model; (b) the block diagram of SDA plant; and (c) the block diagram of the SDA system with a unit feedback and a proportional controller.

3.2. *Fixed end bandwidth*

Let's assume that the actuator output end is fixed. That is, the load velocity $V_L(s)$ is zero in Eq. (2). Then the closed-loop transfer function can be written as:

$$G_{cl} = \frac{F_L(s)}{F_d(s)} = \frac{K_p K_b}{J_m s + B_m + K_b(K_p + 1)}$$

For simplicity, we assume $B_m << K_b(K_p+1)$ and $K_p >> 1$; and define the time constant T as:

$$T = \frac{J_m}{K_b(K_p + 1)} \tag{3}$$

Then we obtain:

$$G_{cl}(S) = \frac{1}{Ts + 1} = \frac{1}{S + 1} \tag{4}$$

where $S = Ts$. It is a first order system and $\frac{1}{T}$ is the SDA system closed-loop bandwidth. From Eq. (3), we see that the system bandwidth can be increased by increasing the damping coefficient K_b and the proportional gain K_p. The frequency response of the SDA system described by Eq. (4) is shown in Fig. 4.

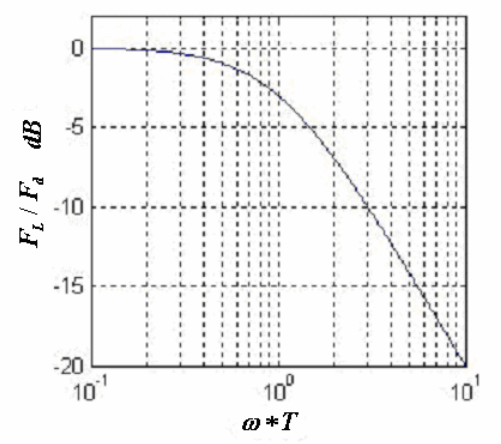

Fig. 4. Fixed end bandwidth of the SDA system with a unit feedback and a proportional controller.

3.3. *Output impedance (for zero reference)*

The output impedance is defined as:

$$Z(s) = \frac{F_e(s)}{X_L(s)}$$

where $X_L(s)$ represents the displacement of the load and $F_e(s)$ ($F_e(s) = -F_L(s)$) represents the external force exerted on the output end of the actuator due to the load.

Assuming $B_m << K_b(K_p + 1)$, the output impedance of the closed loop SDA system with zero force command can be written from Eq. (2) as:

$$Z(s) = K_b \frac{s^2}{Ts + 1} \tag{5}$$

The output impedance of the SDA system is plotted against the frequency as shown in Fig. 5. As illustrated in the figure, the output impedance of the SDA can be very low at low frequency. However, the output impedance of the SDA increases with the frequency. According to Eq. (5), decreasing the damping coefficient K_b or the proportional gain K_p can effectively reduce the system output impedance $Z(s)$.

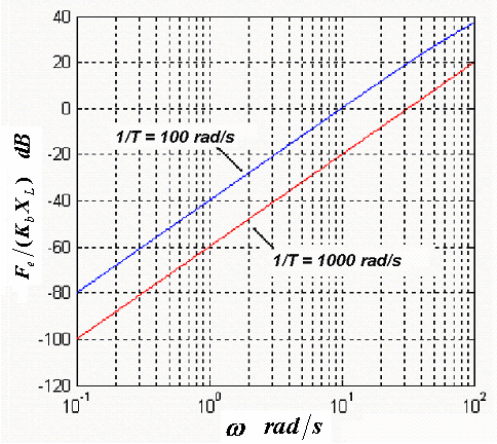

Fig. 5. The output impedance versus the frequency of the SDA system for $\frac{1}{T} = 100$ *rad/s* and $\frac{1}{T} = 1000$ *rad/s*.

4. Controller Design

4.1. *Control scheme*

When we analyze the SDA system in Section 3, we assume a simple proportional controller so that some fundamental properties of the system can be clearly illustrated. To achieve a better force control performance, a PID control scheme is used to control the SDA as shown below in Fig. 6. Furthermore, two feedforward blocks based on the

inverse dynamics model are employed for the reference force and load velocity, respectively. They are intended to improve the system transient response and reduce the effect of the load movement on the output force.

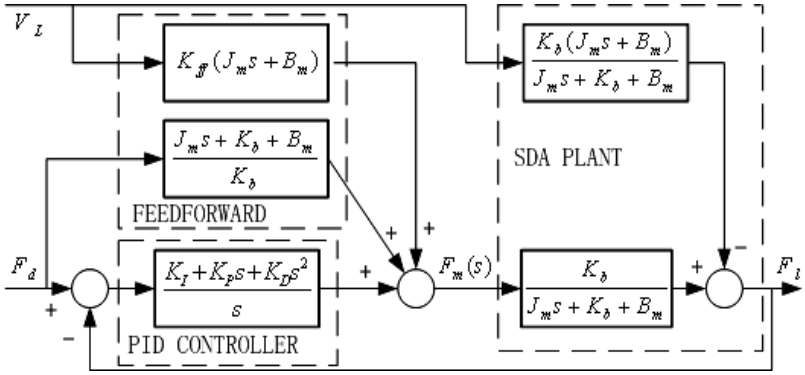

Fig. 6. Control Scheme

4.2. Variable damping coefficient

To achieve variable damping coefficient, we use a Magneto-Rheological (MR) fluid damper (rotary type) as the series damper component. Based on the Bingham viscoplastic model, the dynamics equation of MR damper can be represented as: [12]

$$T = K_d \omega + \{T_f + T(B)\} \cdot sign(\omega) \tag{6}$$

where T is the overall torque; K_d is the damping coefficient when no field is applied; ω is relative angular velocity of the MR damper; T_f is frictional torque; $T(B)$ is the variable torque which is a function of the magnetic flux density B.

The problem with the MR damper is that it does not behave like a linear viscous damper when B is constant. To emulate a linear viscous damper (desirable for the SDA system), a special linearization algorithm is applied to the MR damper. Furthermore, the linearization algorithm can vary the damping coefficient according to the working conditions.

Assuming that $T_f << T(B)$ and $T(B)$ has a linear relationship with the absolute value of the input current for the MR damper, that is, $T(B) = K_a.|I(t)|$, Eq. (6) can be rewritten as:

$$T = K_d \omega + K_a \cdot \left|I(t)\right| \cdot sign(\omega) \tag{7}$$

where K_a is a constant whose value depends on the inherent property of the MR fluid damper. Applying the following linearization algorithm:

$$I(t) = K_c \omega(t) \tag{8}$$

Eq. (7) becomes:

$$T = K_d \omega(t) + K_a K_c \omega(t) = K_b \omega(t) \tag{9}$$

where K_c is the linearization algorithm constant, and:

$$K_b = K_d + K_a K_c \tag{10}$$

When the linearization algorithm is executed, the MR damper behaves like a linear viscous damper with T proportional to ω, and K_b is the effective damping coefficient. From Eq. (10), since K_a and K_d are constants, the damping coefficient K_b of the series damper can modified by changing the value of K_c.

The main difference between the SDA based force control implementation and the existing MR damper based force control implementation [10, 11] is that the latter assumes that the output force is not dependent on the input/output relative velocity of the damper. [10, 11] The drive unit is mainly used to supply a velocity source to one end of the MR fluid damper. The output force is only controlled by the current supply to the MR fluid damper.

For the SDA system, the force control is achieved by controlling the damper's input/output relative velocity. It can use a broad range of dampers, such as linear or nonlinear viscous damper, MR fluid damper, ER fluid damper, or other types of dampers as long as their force output can be a function of the input/output relative velocity (either by virtue of their designs or by software control).

5. Experimental Setup and Results

An experimental setup of the Series Damper Actuator (SDA) and its schematic diagram are shown in Fig. 7 and Fig. 8, respectively. In this experimental system, two angular encoders are used to obtain the series damper input angular velocity and output angular velocity, respectively. The relative angular velocity in the series damper, $\omega(t)$, is calculated from the difference between the two angular velocities.

The series damper component is a Magneto-Rheological Fluid damper (Lord MRB-2107-3) which has a controllable damping coefficient as described in the previous section. A damping coefficient controller is used to control the damping coefficient of the series damper according to the damper's linearization law.

The main controller is implemented on a microcomputer system. It obtains the feedback signals from the two encoders and computes the motor drive signal according to the given control scheme so that the desired force can be achieved at the actuator output. To measure the actual system output torque, a torque sensor is mounted at the end of the

actuator.

The results of the fixed end experiment are shown in Figs. 9 to 13. Fig. 9 and Fig. 10 illustrate the system responses for sinusoidal and step references, respectively, when $K_b = 0.18 Nms$. The results show that the experimental SDA system has no problem in achieving force control.

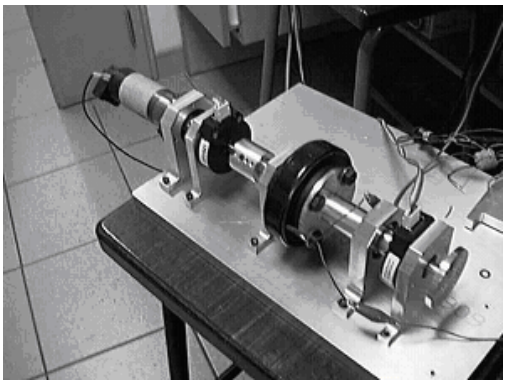

Fig. 7. Photograph of the experimental Series Damper Actuator.

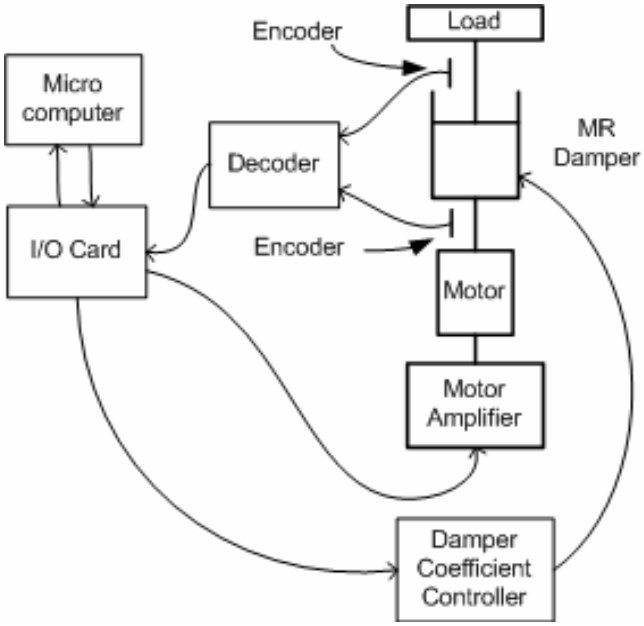

Fig. 8. Schematic diagram of the experimental system

Variable damping coefficient is another advantage of the experimental SDA system. Fig. 11 and Fig. 12 shows the system responses for sinusoidal and step inputs, respectively, after the damping constant K_b has been doubled to $K_b = 0.36Nms$ while the amplitudes of the inputs were increased by four times.

The results demonstrate that the experimental SDA system can maintain its force fidelity at different force ranges by varying the damping coefficient. For example, to achieve higher force output, the damping coefficient should be increased accordingly. This feature greatly eases the design trade-off encountered in the Series Elastic Actuator (SEA) system. In the SEA system, due to the fact that it is difficult to achieve variable series elastic component, one has to trade off between maximum force and bandwidth of the force control.

The experimental SDA system has a bandwidth of around 10 Hz (when the damping constant, $K_d = 0.36Nms$) as shown by the frequency response study (Fig. 13). This is somewhat low compared to the theoretical analysis in Section 3. This problem is mainly contributed by the dynamics of the linearization algorithm which is applied to the MR fluid damper. The analysis of the SDA system is based on an ideal viscous damper whose force is proportional to the relative velocity between the input and output. In the physical experiment, the constitutive property of the MR damper is altered by the linearization algorithm so that it behaves like a linear viscous damper. However, the dynamics of the linearization effort which involves the dynamics of the electromagnetic and mechanical fluid domains[12, 13] is rather significant and it compromises on the bandwidth of the whole system. To achieve a better force bandwidth, we should use a truly viscous damper for the SDA system.

Some comments on this experimental SDA system should be given here. It is known from the analysis in Subsection 3.4 that the SDA system has shock absorption behavior which depends on the effective damping. If the effective damping constant is high, the ability to absorb impact may be limited. However in this experiment, the MR fluid damper used has an inherent “fuse” torque which limits the torque transmission through it. This provides a better impact resistance than the theoretical behavior

In the experimental setup, we have adopted the digital encoders to indirectly measure the damper input and output velocities. From the two values, the relative velocity in the damper can be computed. Other types of velocity measurement devices can also be applied for the SDA system, for example, tachometers, potentiometers, etc. If it is not necessary to measure both the input and output velocities of the damper, we can also have just one velocity sensor to directly measure the relative velocity of the damper.

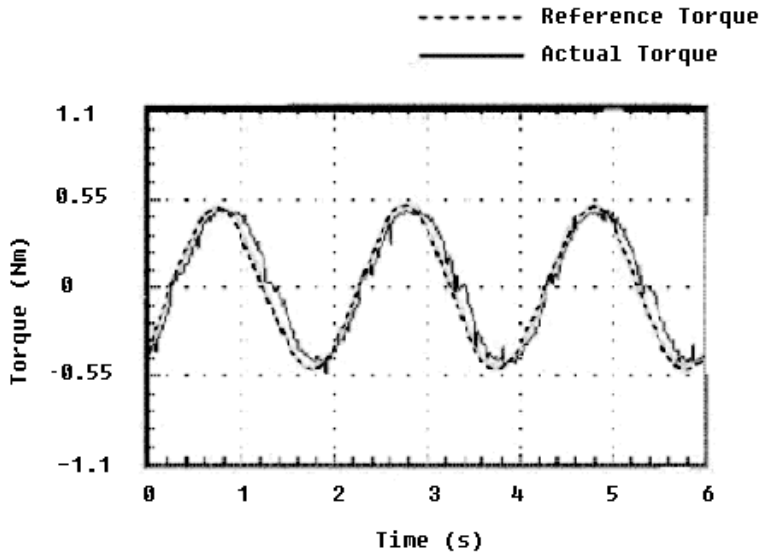

Fig. 9. Force tracking following a sinusoidal reference when the damping constant $K_d = 0.18 Nms$.

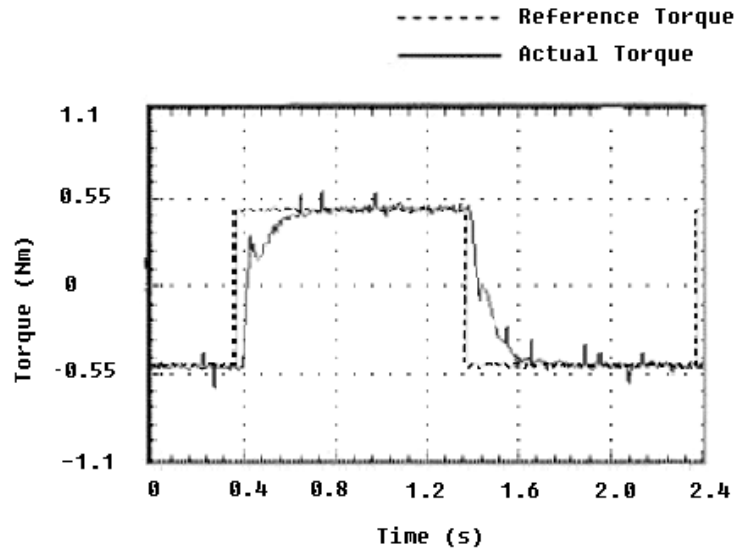

Fig. 10. Force tracking following a step reference when the damping constant $K_d = 0.18 Nms$.

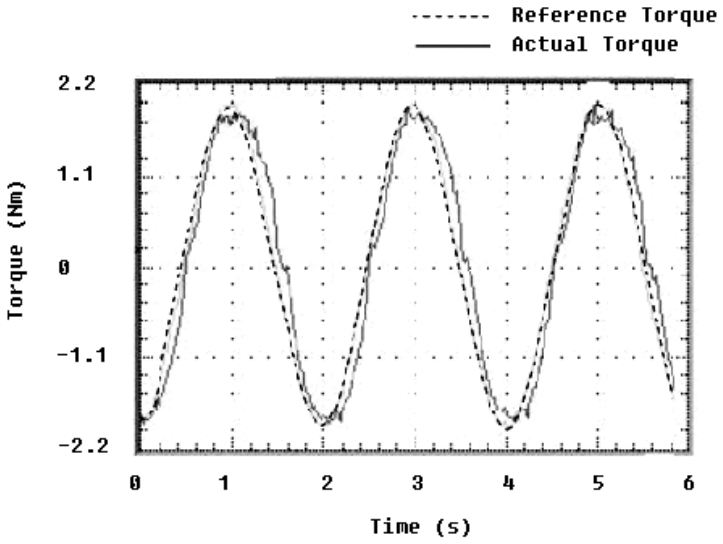

Fig. 11. Force tracking following a sinusoidal reference when the damping constant $K_d = 0.36 Nms$.

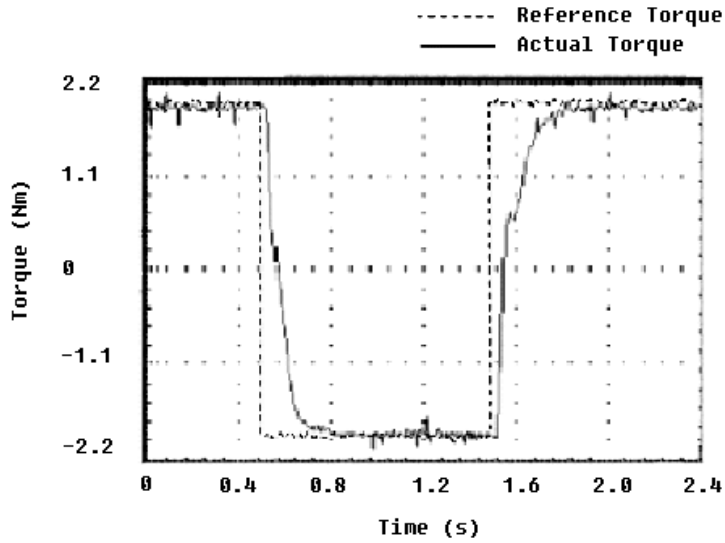

Fig. 12. Force tracking following a step reference when the damping constant $K_d = 0.36 Nms$.

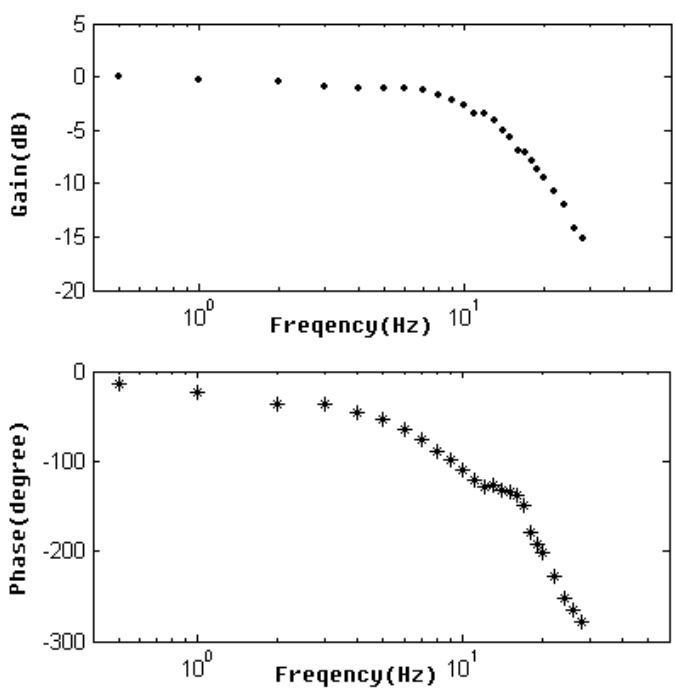

Fig. 13. Frequency response of the experimental SDA system when the damping constant $K_d = 0.36 Nms$.

6. Conclusion and Future Work

In this paper, the Series Damper Actuator, a novel force/torque control actuator is introduced. A first order model of the actuator is used to investigate its force control performance, in particular, the bandwidth and output impedance.

The control scheme and experimental SDA system are also presented. A MR fluid damper is used as the series damper. It is controlled so that it has a linear torque versus velocity relationship and can achieve varying damping coefficient. The fixed end experiment results illustrated that the SDA could achieve force control. By varying the damping coefficient of the series damper, the SDA system was demonstrated to be versatile and applicable for both low and high force output.

The future work would be focused on solving the bandwidth limitation caused by the MR fluid damper. Other types of viscous dampers and damper designs will also be explored to improve the system performance of the SDA system.

Acknowledgements:

This project is funded by the Academic Research Fund of the National University of Singapore.

Reference

1. D. Vischer and O. Khatib, Design and development of high-performance rorque-controlled joints, *IEEE Transactions on Robotics and Automation* **11**.(4), (1995).
2. N. Mandal and S. Payandeh, Force control strategies for compliant and stiff contact: an experimental study, in *IEEE Int. Conf. on Systems, Man, and Cybernetics* (IEEE Press, 1994), pp. 1285-1290.

3. S. Sugano, S. Tsuto and I. Kato, Force control of the robot finger joint equipped with mechanical compliance adjuster, in *IEEE Int. Conf. on Intelligent Robots and Systems (IROS)* (IEEE Press, 1992), pp. 2005-2012.
4. D. W. Robison and J. E. Pratt, Series elastic actuator development for a biomimetic walking robot. in *IEEE/ASME Conf. on Advanced Intelligent Mechatronics* (1999).
5. G. A. Pratt and M. M. Williamson, Series elastic actuators, in *IEEE Int. Conf. on Intelligent Robots and Systems (IROS)* (IEEE Press, 1995), pp. 399-406.
6. S. D. Eppinger and W. P. Seering, Three dynamic problems in robot force control, in *IEEE Int. Conf. on Robotics and Automation (ICRA)* (IEEE Press, 1989), pp. 392-397.
7. Zinn M., Khatib O., Roth B. and Salisbury, J.K.. A New Actuation Approach for Human Friendly Robot Design, in *Int. Symp. on Experimental Robotics* (Italy, 2002).
8. C.-M. Chew, G.-S. Hong and W. Zhou, Series damper actuator for force/torque control, *US Patent Provisional Application*. Application No.: 60/469,825.
9. W. Zhou, C.-M. Chew and G.-S. Hong, Force control characteristics of series damper actuator, *Internal Report of Control and Mechatronics Lab.*, Dept. of Mechanical Engineering, National Univ. of Singapore (2002).
10. N. Takesue, J. Furusho and Y. Kiyota, Analytic and experimental study on fast response MR-fluid actuator. in *IEEE Int. Conf. on Robotics and Automation (ICRA)* (IEEE Press, 2003), pp. 202-207.
11. N. Takesue, H. Asaoka, J. Lin, M. Sakaguchi, G. Zhang and J. Furusho, Development and experiments of actuator using MR fluid, in,.26th Annual Conference of the IEEE Industrial Electronics *(IECON*) (IEEE Press, 2000), pp. 1838 – 1843.
12. J.-H. Kim and J.-H. Oh, Design and analysis of rotary MR damper using permanent magnet. in *2nd IFAC Conference on Mechatronic Systems* (Berkeley, USA, Dec. 9-11, 2002), pp.899-903,.
13. D. Jeon, C. Park and A. Park, Vibration suppression by controlling an MR damper. *International Journal of Modern Physics B* **13**, pp. 2221-2228 (1999).
14. B.F. Spencer Jr., S.J. Dyke, M.K. Sain and J.D. Carlson, Phenomenological model of a magneto-rheological damper. *Journal of Engineering Mechanics*, ASCE, pp. 230-238 (1997).